Probing the Effect of Side Chains on the Conformation and Stability of Helical Peptides via Isotope-Edited Infrared Spectroscopy†

R. A. Gangani D. Silva, Julie Y. Nguyen, and Sean M. Decatur*

Department of Chemistry, Mount Holyoke College, South Hadley, Massachusetts 01075

Received July 24, 2002; Revised Manuscript Received September 18, 2002

ABSTRACT: The mechanism of helix stabilization or destabilization by different amino acids has been the subject of several experimental and theoretical studies; these studies suggest that large or bulky side chains may modulate helix stability by altering the hydration of the helix backbone. In this paper, we report a spectroscopic study to determine the effect of alanine to leucine substitutions on the conformation and solvation of specific segments of a model helical peptide. A 25-residue, alanine-rich, helical peptide [Ac-$(AAAAK)_4$-AAAAY-NH_2 (AKA)] and its two leucine variants [Ac-LLLLK-$(AAAAK)_3$-AAAAY-NH_2 (LKA) and Ac-$(AAAAK)_4$-LLLLY-NH_2 (AKL)] were characterized by infrared (IR) and electronic circular dichroism (ECD) spectroscopies. Introduction of ^{13}C isotopes into specific, consecutive, backbone carbonyls for certain blocks of each of the peptides mentioned above allows the IR spectra to be interpreted in terms of the conformation and solvation of specific residues within the helix. These isotope-edited IR spectra of the leucine peptides do not show evidence of a decrease in the degree of backbone solvation compared to the alanines, but suggest that the peptide may adopt a distorted conformation to accommodate the larger leucine side chains at the N-terminus. These experiments demonstrate the power of isotope-edited IR in dissecting subtle changes in helix conformation at the residue level.

The central problem in biochemistry is the elucidation of the factors responsible for the stability and three-dimensional conformations of proteins. One approach to solving this problem is to study designed model peptides, which isolate particular segments of secondary structure. Because the number of forces and interactions is reduced in these model systems compared to natural proteins, model peptides are more amenable to thorough characterization by experimental and computational methods, yet their behavior still lends some insight into the overall protein folding problem. Short, alanine-based peptides which form stable α-helices in aqueous solution have become canonical models for probing factors governing α-helix formation and stability (*1*−*5*). Such peptides have been used to build a detailed understanding of the relative helix propensities of amino acids (*1*) and interactions between different amino acid side chains (*2*−*5*) and to dissect the capping effects of end groups (*6*).

Baldwin et al. (*7*) have used alanine-based peptides to measure relative helix propensity values via a series of host−guest experiments, in which an alanine residue is replaced with the other 19 naturally occurring amino acids. Though the general trend of relative helix propensities observed in alanine-rich peptides is similar to that observed in studies of globular proteins, the absolute propensities within peptides deviate substantially from protein results; most notably, the helix propensity of alanine is much larger relative to that of glycine in model peptides than in folded proteins (*8*−*10*). In part because of these discrepancies, recent attention has focused on explaining the mechanism by which different amino acid residues stabilize or destabilize helix formation in model peptides.

One factor contributing to helix propensities is conformational entropy of side chains; amino acids with larger side chains lose more conformational entropy than amino acids with smaller side chains (such as alanine), resulting in an entropic barrier to helix formation (*11*−*13*). However, while differences in side chain conformational entropy can explain the general trend of relative helix propensities, it cannot address differences between amino acid propensities in model peptides and in proteins.

Luo and Baldwin (*14*) have proposed that amino acids with bulky hydrophobic side chains (such as leucine) contribute to the desolvation of the peptide backbone by disrupting hydrogen bonding between backbone atoms and surrounding water; this desolvation may be responsible for a smaller enthalpy change upon helix formation in the leucine-containing peptides than in alanine-containing peptides. Calculations of electrostatic solvation free energies (ESFs) in alanine peptides with single-site substitutions of bulky nonpolar residues are consistent with this model; the calculated changes in ESF upon substitution of alanine with nonpolar bulkier residues are comparable in size to the experimentally measured helix propensities (*15*). These experimental and theoretical results point toward side chain shielding as a major contributor to helix propensities.

Others have proposed that water−backbone hydrogen bonding may be particularly important in these soluble alanine-rich peptides, resulting in a larger helix propensity of alanine in these peptides than in proteins. Scheraga and

† This work was supported by grants from Mount Holyoke College, the National Science Foundation (CHE99848444), and the National Institutes of Health (R15GM54334).

* To whom correspondence should be addressed. Phone: (413) 538-2115. Fax: (413) 538-2327. E-mail: sdecatur@mtholyoke.edu.

10.1021/bi026507z CCC: $22.00
Published on Web 12/03/2002

co-workers (*16*) recently reported results of conformational energy calculations on alanine-based peptides in which polar side chains reduce the degree of solvation of backbone CO and NH groups by bulk water, inducing formation of intrahelical hydrogen bonds. These results are consistent with an all-atom simulation of the helix−coil transition in a helical peptide (*17*), which predicts that arginine side chains in a model peptide reduce the water coordination of selected residues by 50%, resulting in a stabilization of the overall helix.

Thus, experimental and theoretical evidence points toward modulation of backbone−water hydrogen bonding by side chains as a major determinant of helix propensities. However, there has been no direct spectroscopic evidence indicating either a change in backbone hydration or local helix backbone rearrangement in response to side chain substitutions within these helical peptides. Characterization of local changes in the conformation of the polypeptide backbone and interactions with solvent upon amino acid substitution would help in sorting through these different models of helix stabilization by amino acid side chains.

The conformation of helical peptides has been probed by a wide range of spectroscopic techniques, including electronic circular dichroism (ECD) (*2*, *18*), nuclear magnetic resonance (NMR) (*4*, *19*, *20*), infrared (IR) spectroscopy (*21*−*26*), and vibrational circular dichroism (VCD) (*27*, *28*). While ECD is sensitive to the overall secondary structure content of the peptide, the spectra do not give information about the conformation of specific residues. Thus, while ECD is an effective tool for determining the effect of an amino acid substitution on the stability of a model helix, it cannot elucidate the impact of the substitution on local structure. NMR can provide information about specific residues within the peptide, but the difficulties of assigning spectra of alanine repeat sequences combined with the fast kinetics of peptide conformational interconversions compared to the time scale of NMR observation can obscure results (*29*).

Vibrational techniques, such as IR spectroscopy, focus primarily on the amide I mode. The amide I band arises mainly from the stretching of backbone carbonyls of the polypeptide. Due to transition dipole coupling and intrapeptide hydrogen bonding, the amide I mode is very sensitive to the secondary structure of the peptide, and the features of this band (frequency, intensity, and bandwidth) can be used to probe the backbone conformation (*30*−*32*). IR and VCD are generally considered low-resolution approaches to peptide conformation, similar to ECD. However, via introduction of specific isotope labels into the peptide backbone, spectral features arising from those specific resides can be resolved and used as probes for conformation at the residue level (*25*, *26*, *28*, *33*−*36*). Labeling a backbone carbonyl with ^{13}C shifts the amide I band of the labeled residue to a lower frequency, allowing the ^{13}C amide I band to be observed outside of the ^{12}C band envelope. This approach of "isotope-edited" IR has been applied in dissecting the conformation of alanine-based helical peptides. In these studies, ^{13}C-substituted alanines were incorporated at different positions in the peptide; the isotope-shifted ^{13}C amide I mode was then used to probe the conformation of the peptides at the residue level (*26*, *28*, *33*, *35*), to determine the effect of N-acetylation on the conformation of specific residues of the peptide (*25*), and to observe the kinetics of helix formation at the residue level (*34*, *36*).

Table 1: Peptide Sequences and Their Abbreviations[a]

sequence	abbreviation
Ac-AAAAKAAAAKAAAAKAAAAKAAAAY-NH_2	AKA
Ac-LLLLKAAAAKAAAAKAAAAKAAAAY-NH_2	LKA
Ac-AAAAKAAAAKAAAAKAAAAKLLLLY-NH_2	AKL
Ac-**AAAA**KAAAAKAAAAKAAAAKAAAAY-NH_2	$\underline{A}$KA
Ac-**LLLL**KAAAAKAAAAKAAAAKAAAAY-NH_2	$\underline{L}$KA
Ac-$\bar{A}\bar{A}\bar{A}\bar{A}$KAAAAKAAAAKAAAAK**AAAA**Y-NH_2	$\bar{A}$KA
Ac-AAAAKAAAAKAAAAKAAAAK**LLLL**Y-NH_2	AK$\underline{L}$
Ac-AAAAK**AAAA**KAAAAKAAAAK$\bar{A}\bar{A}\bar{A}\bar{A}$Y-$NH_2$	AA$\bar{A}$KA
Ac-LLLLK**AAAA**KAAAAKAAAAKAAAAY-NH_2	L$\underline{A}$KA

[a] Note that the ^{13}C substitutions are at backbone carbonyl carbons, and amino acids bearing such carbonyls are denoted as bold, underlined letters.

IR spectroscopy combined with specific isotope labeling seems particularly well suited for dissecting the effects of side chains on the conformation and stability of helical peptides. Not only is the amide I band of peptide sensitive to the backbone conformation (*30*−*32*), but it also is affected by changes in the hydration of the backbone; dehydration of the helix backbone results in a shift of the helical amide I mode to a higher frequency (*21*, *37*, *38*). Thus, by probing the effects of alanine to leucine substitutions in model peptides with isotope-edited IR, one can not only measure the effect of the substitution of helix stability but also detect subtle changes in the conformation and hydration of the peptide backbone caused by the change in side chain structure. In this paper, we report a spectroscopic analysis of a 25-residue, water soluble, alanine-rich peptide and selected leucine variants. We have used conventional IR and ECD spectra of the unlabeled peptides to obtain information about the overall stability. In addition, a comparative analysis of IR spectra of specifically labeled peptides was used to probe the effect of alanine to leucine substitutions on the conformation of specific segments of the peptide.

MATERIALS AND METHODS

Nine 25-residue α-helical peptides, based on the AAKAA repeating unit (*1*) (Table 1), were used in the study. The peptides are consistent with blocks of similar segments, and each time, four consecutive amino acids were labeled with ^{13}C to gain sufficiently intense IR absorption amide I signals from these labeled carbonyls. The peptides were synthesized according to standard techniques of 9-fluorenylmethyloxycarbonyl (Fmoc) chemistry on a Perseptive Biosystems Pioneer automated peptide synthesizer, and purified by reverse phase HPLC (Pharmacia Biotech, Vydac C18 column). The correct mass and the presence of the ^{13}C labels in isotopically labeled peptides were identified by electrospray mass spectrometry and were found to be within 0.5 amu of their calculated molecular weights. The peptide samples were exchanged with a mixture of D_3PO_4 in D_2O (0.1%, v/v) and freeze-dried overnight until they were completely dry. This step was carried out to remove residual trifluoroacetic acid (TFA) anion resulting from the peptide cleavage step, which would otherwise partially interfere with the spectrum of the peptide with its strong absorbance at ∼1673 cm^{-1}. This step also lets all exchangeable H's in the peptide be replaced by deuterium which results in an ∼5−

10 cm^{-1} shift of the amide I band to a lower frequency; this band is termed amide I′ when measured in D_2O (*39*). Complete H−D exchange can be confirmed by the disappearance of the amide II band at 1525 cm^{-1} and also by the identical frequency positions of the IR absorption amide I′ bands at 1.6 °C before and after going through the heating process.

Freeze-dried samples were dissolved in fresh D_2O, and the IR spectra were collected in the temperature range of 1.6−73.3 °C nearly every 5 °C using a Bruker (Vector 22) FTIR absorption spectrometer. Once the sample solutions reached the required temperature, they were equilibrated for 15 min before data were collected. The spectra recorded with a DTGS detector were collected with 4 cm^{-1} resolution and are averages of 1024 scans. The sample solutions were placed in a Wilmad temperature-controlled cell equipped with CaF_2 windows, separated by an ∼50 μm spacer attached to a Neslab (RTE-110) water circulating bath. The temperature at the cell, very close to the sample solution, was monitored with an external thermometer (Barnant) equipped with a thermocouple (Omega Engineering Inc.) which is accurate up to 0.1 °C. The path length of the spacer was estimated by measuring the interference fringe pattern corresponding to the transmittance of the empty cell, and typically ranged from 41 to 48 μm. The solvent correction was done by subtracting spectra of D_2O at each temperature from measured sample spectra with the same spacer used for a set of sample measurements. The concentrations of the peptide sample solutions were determined by UV absorption of Tyr at 275 nm (ϵ = 1450 M^{-1} cm^{-1}) located at C-terminus of each peptide. Since such model peptides were shown to have unordered C-termini (*25*, *26*, *28*, *34*, *35*), the Tyr absorbances were recorded with dilute peptide solutions without denaturing the peptides. The sample concentrations used for IR measurements were within 7−9 mM and were completely soluble under these conditions (*1*). The amide I′ frequency positions were fully reproducible once the sample solution had cooled to 1.6 °C after going through the heating process.

ECD spectra of the peptides were collected from 280 to 185 nm (wavelength range) every 5 °C, with a time constant of 100 ms using an Aviv 215 ECD spectrometer, equipped with a Peltier temperature-controlled cell jacket. Samples were equilibrated for 10 min at each temperature before scans were collected. The dynode voltage was maintained below 500 V throughout the measurements. Concentrations of the peptide solutions used to measure ECD (∼0.06 mM per peptide) were calculated just as was described for IR samples. The spectra were converted to molar ellipticity units after subtraction of baseline of just water measured at 25 °C (since there is no baseline fluctuation observed with the change in temperature).

RESULTS

ECD Spectroscopy. ECD spectra of AKA, LKA, and AKL (Table 1), in the far-UV region (260−185 nm), recorded with ∼0.06 mM peptide at 0 °C are given in Figure 1a. These spectra consist of a double minimum (∼208 and ∼222 nm) and an intense maximum (∼195 nm) which are of typical α-helical spectral features and an intensity indicating a very high percentage of peptide residues in the helical conformation. The α-helix contents of these model peptides at 0 °C

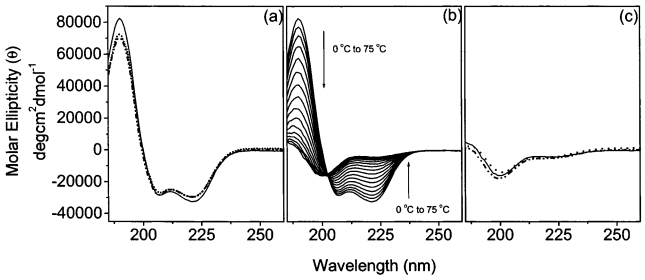

FIGURE 1: ECD spectra of (a) AKA (—), LKA (••—••), and AKL (•••) at 0 °C, (b) AKA in the temperature range of 0−75 °C every 5 °C, and (c) AKA (—), LKA (••—••), and AKL (•••) at 75 °C. The spectra were recorded with ∼0.06 mM peptide and a path length of 1 mm.

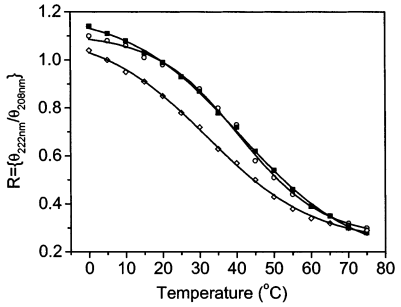

FIGURE 2: Comparison of melting behaviors of AKA (■), LKA (◇), and AKL (○) using the ECD spectral intensity ratio of two minima at ∼222 and ∼208 nm (denoted as *R*) calculated for each measurement from 0 to 75 °C every 5 °C. Melting temperatures for each peptide were obtained after subjecting each data set to nonlinear sigmoidal fitting (∼41.8 °C for AKA, ∼34.9 °C for LKA, and ∼44.5 °C for AKL).

are very similar, as reflected by small differences in molar ellipticity ([θ]) at ∼222 nm among AKA (∼32310), LKA (∼28860), and AKL (∼30620). Another quantitative method of comparing helicity via ECD spectra is to use *R* values, where $R = \theta_{(222\ nm)}/\theta_{(208\ nm)}$. *R* values have been used extensively to distinguish between α- and 3_{10}-helices using ECD spectra (*40*, *41*). The *R* values for all three peptides are greater than 1 (1.14 for AKA, 1.10 for LKA, and 1.04 for AKL), consistent with an α-helical conformation.

The melting pattern is shown for AKA within the range of 0−75 °C range every 5 °C (Figure 1b). All three peptides exhibit evidence of a gradual helix to coil conformational transition, with the only significant feature in the unordered spectra at high temperatures being a broad weak negative signal at ∼200 nm (Figure 1c) which is typical for a peptide in an unordered conformation.

Differences in the stability of the three peptides are made clearer in their melting curves. Plots of *R* values versus temperature for AKA, LKA, and AKL in the temperature range of 0−75 °C (Figure 2) clearly show that replacement of four alanines with leucines at the N-terminus (LKA, Table 1) results in a lower melting temperature (∼34.8 °C) than in AKA (∼41.8 °C), while replacement of alanines with leucines at the C-terminus (AKL, Table 1) gives a slight increase in melting temperature (∼44.5 °C).

IR Spectroscopy of Unlabeled Peptides. The amide I′ bands for AKA, LKA, and AKL (Table 1) at 1.6 °C (Figure 3a) are remarkably similar. All three peptides have amide I′ frequencies in the range of 1631.5−1632.1 cm^{-1}, which are typical for solvent-exposed α-helices in D_2O at low tem-

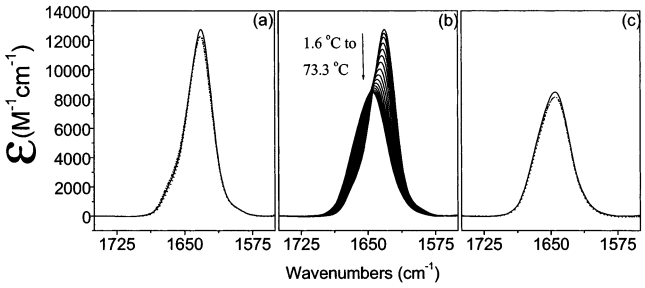

FIGURE 3: Overlay of IR absorbance amide I′ bands of (a) AKA (—), LKA (••—••), and AKL (•••) at 1.6 °C, (b) temperature-dependent spectra of AKA from 1.6 to 73.3 °C nearly every 5 °C, and (c) AKA (—), LKA (••—••), and AKL (•••) at 73.3 °C. Note that the spectra are expressed in molar absorptivity units independent of the sample concentration (~7 mM) and path length (~50 μm) which were determined accurately for each set of measurements.

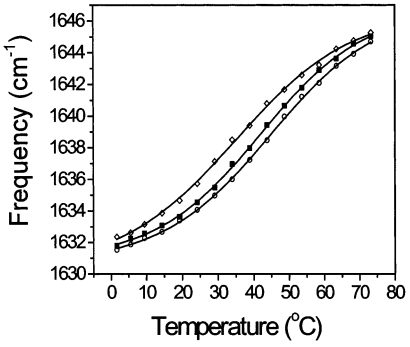

FIGURE 4: Plot of frequency positions of the original IR absorption amide I′ bands vs temperature (1.6−73.3 °C, nearly every 5 °C) for AKA (■), LKA (◇), and AKL (○) peptides. Each data set was fit with a sigmoidal function (melting temperatures of ~42.8 °C for AKA, ~35.8 °C for LKA, and ~45.7 °C for AKL).

peratures (*22*, *24*−*28*, *34*, *35*).[1] With an increase in temperature, the amide I′ band gradually shifts to higher frequencies while broadening and decreasing in intensity (shown for AKA, Figure 3b). By 73.3 °C, all peptides have amide I′ frequencies within the range expected for a peptide in a random coil conformation (1644.7−1645.0 cm^{-1}) (Figure 3c). This helix−coil transition has been observed in the IR with similar sequences (*25*, *26*, *28*). Upon repeated measurements with fresh samples, the frequency positions of the IR absorption amide I′ band for a particular peptide for a given temperature are reproduced within ±0.2 cm^{-1} with the intensities reproduced within ±5%. The plot of frequency positions of the IR absorption amide I′ bands of the three peptides with increasing temperature (Figure 4) reveals the same pattern of melting temperatures that was observed with ECD: LKA (~35.8 °C) has a lower melting temperature than AKA (~42.8 °C), while the melting temperature for AKL (~45.7 °C) is slightly higher.

IR Spectroscopy of ^{13}C-Labeled Peptides. To probe the effect of the alanine to leucine substitutions on local conformation, site specific ^{13}C labels were introduced into the peptides. ECD spectra of the labeled peptides were recorded, and the spectra and melting temperatures of the labeled peptides were similar to those of their unlabeled counterparts (data not shown). Thus, the introduction of ^{13}C labels does not affect the stability or conformation of the helical peptides.

(1) AKA versus LKA. When four consecutive N-terminal backbone carbonyls in AKA and LKA are substituted with ^{13}C (AKA and LKA, Table 1), the amide I′ band shapes at 1.6 °C change considerably from those of unlabeled variants (Figure 5a,b). The amide I′ band of each labeled peptide now consists of two overlapping bands: an intense band due to regular ^{12}C carbonyl vibrations and a less intense sideband ~37 cm^{-1} lower in frequency from the ^{12}C band due to ^{13}C carbonyl vibrations. The spectra of both AKA and LKA have ^{12}C bands at a frequency (~1633.7 cm^{-1}) slightly higher than those of unlabeled peptides (Table 2). While AKA has a well-separated intense sideband, the ^{13}C band of LKA is a less intense, broad shoulder. The intensity of the lowest-temperature LKA spectrum at 1595 cm^{-1} (~3000 M^{-1} cm^{-1}) is smaller than that of AKA (~3840 M^{-1} cm^{-1}); the area of the ^{13}C amide I′ band in LKA (~67570 M^{-1} cm^{-2}), as determined by band fitting to a sum of Gaussians, is also much smaller than that of AKA (~104670 M^{-1} cm^{-2}). Moreover, after the original IR absorption bands were subjected to Fourier self-deconvolution (FSD), second-derivative or difference spectra (subtracting spectra at different temperatures from the highest-temperature spectrum for a specific sequence), it is clearly seen that the LKA sideband is ~1−2 cm^{-1} lower in frequency than that of AKA (Figure 6). IR spectra of AKA and LKA in the temperature range of 1.6−73.3 °C (Figure 5a,b) show that both ^{12}C and ^{13}C amide I′ band frequencies shift to higher frequencies, decrease in intensity, and broaden with increasing temperatures. The remarkable differences in the sidebands at lower temperatures disappear, and both peptides acquire very similar overall band shapes at higher temperatures.

The ^{13}C amide I′ bands and the effects of the ^{13}C labels on the ^{12}C bands are clearly visualized from the difference spectra obtained by subtracting the spectra of unlabeled variants from the spectra of their corresponding labeled variants (Figure 5c,d). Both peptides have sharp positive (~1597 cm^{-1}) and negative (~1627 cm^{-1}) spectral features at the lowest temperature, 1.6 °C. The positive feature can be attributed to the ^{13}C amide I′ band of the labeled peptide. The intense negative feature is indicative of a decrease in the helical ^{12}C bands of the labeled peptides compared to their unlabeled variants. The negative feature, at low temperatures, is centered at 1627 cm^{-1} and shifts to 1642−1644 cm^{-1} at higher temperatures; this reflects the helical conformation of the labeled residues at low temperatures, and the random coil conformation at higher temperatures.

(2) AKA versus AKL. Similar labeling of four consecutive C-terminal carbonyl carbons of AKA and AKL (abbreviated as AKA and AKL, Table 1) also have some amide I′ band shape differences compared to their corresponding unlabeled variants (Figure 7a,b). Unlike the N-terminally labeled peptides, the ^{13}C sidebands are not well-resolved in these C-terminally labeled peptides, appearing as tails to the low-frequency side of the main amide I′ bands. The ^{12}C amide I′ band is not shifted from its position in the unlabeled peptides (~1632 cm^{-1}, Table 2). AKA and AKL spectra both have very similar band shapes as well as frequency positions for ^{12}C as well as ^{13}C bands (as seen from second-derivative, FSD, and difference spectra, data not shown) even at the lowest temperature. The bands in both AKA and AKL shift

[1] Solvent-exposed helices give frequencies that are lower than the characteristic frequencies for α-helices within globular or membrane proteins, which lie in the range of 1650−1660 cm^{-1} (*21*).

Table 2: IR Absorption Amide I′ Frequency Positions of Original and Difference Spectra at 1.6 °C

peptide	^{12}C amide I′ frequency in cm^{-1} (ϵ in M^{-1} cm^{-1})	^{13}C amide I′ frequency in cm^{-1} (ϵ in M^{-1} cm^{-1})	negative lobe of difference[a] spectra frequency in cm^{-1}	positive lobe of difference[a] spectra frequency in cm^{-1}
AKA	1631.5 (~12730)	–	–	–
LKA	1631.5 (~12220)	–	–	–
AKL	1632.1 (~12690)	–	–	–
A̲KA	1633.6 (~10370)	1597.9 (~3840)	1626.4	1596.7
L̲KA	1633.7 (~10670)	shoulder (~3000)[b]	1627.0	1595.9
ĀKA	1631.6 (~11400)	tail (~2740)[b]	1629.5, 1643	1600.8
AK̲L̲	1631.7 (~11510)	tail (~2720)[b]	1628.2, 1643	1600.6
AA̲K̄A	1636.3 (~10640)	1598.6 (~4960)	1627.8	1597.7
LĀK̲A	1636.5 (~10300)	1598.7 (~4580)	1627.6	1597.4

[a] The difference spectra were obtained by subtracting the spectra of the unlabeled peptide from the spectra of their corresponding labeled variants. [b] Frequency positions of unresolved bands were determined from the FSD spectra.

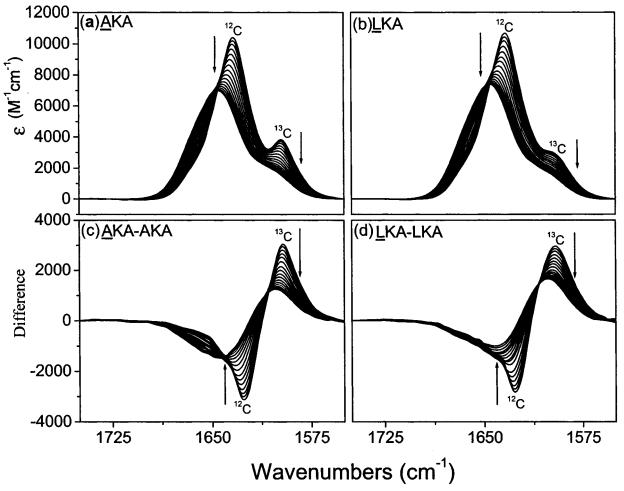

FIGURE 5: IR absorption amide I′ bands in the 1750−1550 cm^{-1} region for A̲KA (a), L̲KA (b), and the difference spectra of A̲KA minus AK̄A (c) and L̲KA minus LKA (d) in the temperature range of 1.6−73.3 °C nearly every 5 °C. Spectral processing was as described in the legend of Figure 3. The arrows indicate the direction of spectral changes with the increase in temperature.

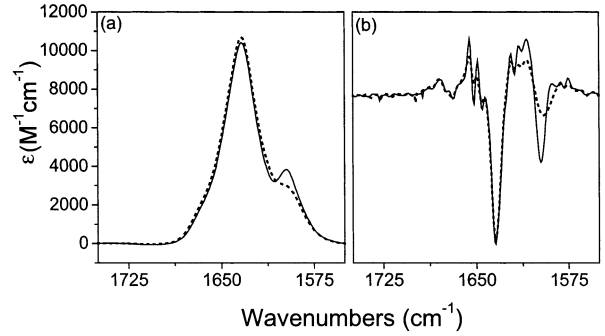

FIGURE 6: Original IR absorption amide I′ bands (a) and the second-derivative spectra (b) of A̲KA (—) and L̲KA (- - -).

to higher frequencies and decrease in intensity with increasing temperatures (Figure 7a,b). The low-temperature labeled minus unlabeled difference spectra for AK̲A̲ and AK̲L̲ (Figure 7c,d) have a positive feature at ~1601 cm^{-1} and two negative features at ~1628 and ~1643 cm^{-1}. The positive feature is the ^{13}C amide I′ band of the labeled peptides; the negative features represent the loss of intensity in the helical (~1628 cm^{-1}) and coil (~1643 cm^{-1}) bands of the ^{12}C amide I′ envelope. The large negative feature at 1643 cm^{-1} in the low-temperature spectrum confirms that the labeled residues are predominantly coil even at this lowest temperature. The change in difference spectral band shapes with an increase in temperature is mainly the decrease in the negative intensity of the ~1630 cm^{-1} band and broadening of the ~1645 cm^{-1} band.

(3) AA̲KA versus LA̲KA. To assess the effect of the alanine to leucine N-terminal substitutions on the conformation of the adjacent segment of the peptides, four consecutive backbone carbonyls in the middle segment closer to the N-terminus in AKA and LKA sequences were labeled (named AA̲KA and LA̲KA, Table 1). The IR spectra at 1.6 °C for both AA̲KA and LA̲KA feature two amide I′ bands originating from ^{12}C and ^{13}C vibrations as seen for other labeled peptides (data not shown). The ^{13}C bands for both peptides are well-resolved at low temperatures, and they are remarkably similar in frequency (~1598.7 cm^{-1}) and intensity (4930 M^{-1} cm^{-1} for AA̲KA and 4590 M^{-1} cm^{-1} for LA̲KA). The labeled minus unlabeled difference spectra at low temperatures have a strong positive feature at ~1597 cm^{-1} and a strong negative feature at ~1627 cm^{-1} (data not shown), reflecting the gain of helical ^{13}C amide I′ intensity and the loss of ^{12}C helical amide I′ intensity in the labeled peptides. These difference spectra also show a small positive feature at ~1645 cm^{-1}. The lack of a negative feature at ~1640−1645 cm^{-1} in these lowest-temperature difference spectra, unlike for the other sets of difference spectra (Figures 5 and 7), indicates the labeled segments of AA̲KA and LA̲KA are strictly helical. The temperature dependence of the IR spectra of both peptides shows very similar melting behavior according to simple frequency analyses (data not shown). These data clearly indicate that the middle segments of AA̲KA and LA̲KA closer to N are similar in conformation and stability.

DISCUSSION

Effect of Alanine to Leucine Substitutions on the Peptide Stability at the N-Terminus. The melting curves for the three unlabeled peptides based on ECD *R* values and FTIR amide I′ frequencies indicate that the leucine substitutions at the N-terminus (LKA) have a destabilizing effect (resulting in an ~7 °C decrease in melting temperature). In previous studies, *R* values have been used as an empirical guide for determining the α-helix content based on ECD spectra (*40*−*42*); this study suggests that *R* values can be a useful probe for comparing helix−coil transitions in peptides of the same length and similar sequence. For each peptide, the melting temperature obtained from FTIR data agrees within 1 °C with those of 100-fold lower concentration ECD. In short,

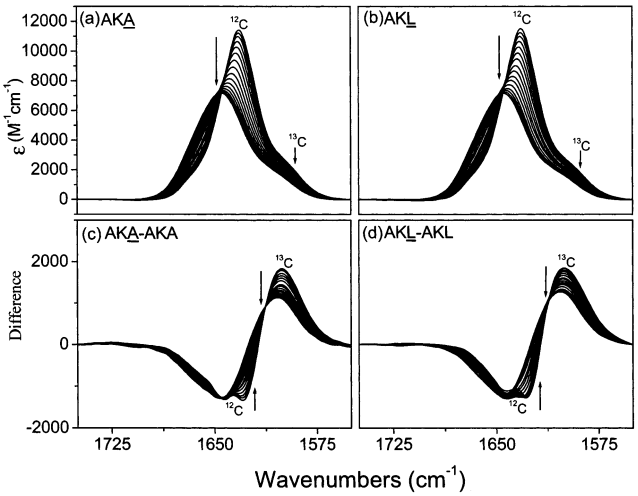

FIGURE 7: IR absorption amide I′ bands in the 1750−1550 cm^{-1} region for AKA (a), AKL (b), and the difference spectra of AKA minus AKA (c) and AKL minus AKL (d) in the temperature range of 1.6−73.3 °C nearly every 5 °C. Spectral processing was as described in the legend of Figure 3.

N-terminal residues of the N-acetylated peptides are predominantly in a helical conformation, while the C-terminal residues are highly frayed (*25*, *26*, *28*, *34*, *35*). Thus, substitution of leucines (which has a lower helix propensity than alanine) at the N-terminus has a significant destabilizing effect on the helix, while the "floppier" C-terminus is more tolerant of substitution.

Effect of Leucine Substitutions on the Conformation of Peptides at the N-Terminus. Overall, the most striking observation about the low-temperature FTIR and ECD spectra of AKA, LKA, and AKL is their remarkable similarity. The amide I′ bands are at ∼1631.5 cm^{-1} for AKA and AKL and at 1632.1 cm^{-1} for LKA at 1.6 °C, consistent with other short model helical peptides at low temperatures (*22*, *24*−*28*, *34*, *35*). These bands also have very similar intensities (Table 2) and line widths. Moreover, the ECD spectra of all three peptides have similar band shapes (Figure 1a). Although the leucine substitutions result in a decrease in helix stability, these spectroscopic approaches cannot detect any significant differences in conformation due to the presence of the leucines. Thus, even though both IR and ECD give very reliable and important information about the overall differences in peptide stability, extraction of any segment specific conformational information is impossible.

When ^{13}C labels are introduced into the peptides, subtle differences in the spectra emerge. ^{13}C amide I′ bands of AKA and LKA at low temperatures are significantly different in intensity, frequency, and area; the ^{13}C amide I′ band of LKA is significantly decreased in intensity and shifted to a lower frequency by 1−2 cm^{-1} (Figure 6 and Table 2). Since the features of the ^{13}C amide I′ band reflect the conformation and solvation of the labeled segment of the peptide, these spectra indicate structural differences at the N-terminus in AKA and LKA.

The identical frequencies, intensities (Table 2), and areas of the ^{13}C amide I′ bands of the pair of peptides (AAKA and LAKA) prove that the conformation is identical at the labeled sites. This suggests that the structural differences caused by the alanine to leucine substitutions at the N-terminus do not extend to the adjacent residues in the helix. Thus, these alanine to leucine substitutions result in a change in backbone conformation or environment which is *local* to the site of substitution.

The frequency and band shape differences observed between AKA and LKA are not consistent with a reduction in the extent of water−backbone hydrogen bonding at these positions. Previous studies have demonstrated that dehydration of the peptide backbone [either by burial within a hydrophobic interior (*37*) or as induced by trifluoroethanol (*38*)] results in an amide I′ band shift to a *higher* frequency. Thus, while there are clear spectroscopic differences between AKA and LKA (including a shift of the amide I′ to a *lower* frequency), other conformational changes besides a reduction in the extent of solvent−backbone hydrogen bonding must be occurring at the site of the substitutions.

The decrease in frequency and intensity of the ^{13}C amide I′ band may arise from a change in the backbone conformation at the site of the labeled residues. Because the coupling between amide I′ modes is dependent on the relative geometries of adjacent carbonyls, subtle changes in the conformation of the polypeptide backbone will result in changes in the observed amide I′ frequency. One possibility would be a fraying of the N-terminus brought on by the presence of the leucine side chains. However, the changes observed in the ^{13}C amide I′ band of LKA compared to that of AKA are not consistent with simple fraying of the N-terminus; when the N-terminus is frayed (with residues primarily in random coil, as in a helical peptide lacking an N-capping acetyl group), the ^{13}C amide I′ band has a larger decrease in intensity and shifts to a higher frequency (*25*).

Thus, spectroscopic data suggest that the leucines at the N-terminus of LKA are not simply dehydrating or unwinding compared to N-terminal alanines in AKA. An alternate explanation is that the leucine side chains distort the conformation of the helix backbone; distortion of the helix backbone away from the standard α-helix (ϕ and ψ) angles toward a 3_{10}-helix conformation may make it easier to accommodate the leucine side chains in LKA and may result in favorable hydrophobic interactions between the side chains (*43*). In proteins, α-helices commonly form 3_{10}-structures at the termini, and in model peptides, 3_{10}-helices have been proposed as intermediates to α-helix formation (*44*, *45*). On the basis of the frequency of occurrence in 85 nonhomologous globular proteins, Thornton et al. deduced that leucine has a higher propensity for 3_{10}-helix formation than alanine (*46*); perhaps this makes the adjacent leucines more likely to adopt a 3_{10}-conformation at the N-terminus than alanine (*47*).

Distortion of the N-terminus of LKA to a 3_{10}-like conformation is consistent with the observed IR spectral changes. Ab initio models of polypeptide IR spectra predict that distortion of the α-helix backbone to a 3_{10}-helix should result in a decrease in the frequency of the amide I band (*48*). The same trend is found in a coupled oscillator model of amide I frequencies in globular proteins, in which elongation of the helix (i.e., moving from an α-helix to a 3_{10}-conformation) results in a shift to a lower frequency (*49*, *50*). Thus, we conclude that the N-terminus of LKA adopts a 3_{10}-conformation, while the N-terminus of AKA is α-helical.

Effect of Leucine Substitutions on the Stability and Conformation at the C-Terminus. The peptides AKA and

AKL are remarkably similar in their melting curves and their spectra. According to both IR and ECD melting curves, the leucine substitutions at the C-terminus (AKL) are weakly stabilizing, resulting in an ~3 °C increase in the melting temperature. This is consistent with recent observations in the literature (*51*), in which leucine is found to be a weakly stabilizing amino acid when substituted near the C-terminus of a model peptide. The low-temperature IR spectra of the labeled peptides AK$\underline{A}$ and AK$\underline{L}$ also look very similar; in both cases, the ^{13}C sideband is poorly resolved, appearing as a tail to the larger ^{12}C band. Moreover, the frequency of this band does not change significantly with temperature. These spectra are consistent with previous studies of labeled peptides and are likely due to significant fraying of the helix at the C-terminus (*25*, *26*, *28*, *34*, *35*). Since the C-terminus is already frayed, it is more tolerant to substitution than the highly helical N-terminus, and thus, the alanine to leucine substitutions result in no detectable changes in conformation.

CONCLUSIONS

Substituting leucine for alanine at the N-terminus of the alanine-rich helical peptides results in destabilization of the helix. Using specific ^{13}C labeling of the peptide backbone, we conclude that these substitutions result in a subtle rearrangement of the peptide backbone at the site of the leucine substitution. We do not find any evidence for a reduction in the extent of solvent−backbone hydrogen bonding due to shielding by the leucine side chains; thus, the smaller helix propensity of leucine relative to that of alanine measured in these model peptides may be due to its effect on the local backbone conformation as opposed to modulation of water−backbone hydrogen bonding. One possible change is that the N-terminus of the helix becomes more elongated and tightly coiled in LKA relative to that in AKA, resulting in a mixed $3_{10}/\alpha$-helix system. The changes brought about by the leucines in LKA are strictly local; there is no change in the amide I′ bands arising form the alanines adjacent in sequence.

These data demonstrate the value of using site specific ^{13}C labeling in conjunction with IR spectroscopy to gain information about the backbone conformation of specific segments of model peptides. No significant differences are observed in the IR and ECD spectra of the unlabeled peptides that were studied (AKA, LKA, and AKL), but careful analysis of the isotope-edited IR spectra results in important differences as a function of residue position and local amino acid composition. Further, characterization of model helices by isotope-edited IR, combined with theoretical modeling of spectra, will be a valuable tool in determining the impact of specific amino acids on helix conformation. This approach may prove to be valuable in dissecting conformational changes and dynamics in other peptides and proteins. These studies may be particularly useful for systems typically not accessible to study by NMR, such as fast conformational changes or membrane proteins.

ACKNOWLEDGMENT

We thank Ms. Wendy Barber-Armstrong for assistance and Dr. Stephen Eyles for help with mass spectrometry.

REFERENCES

1. Marqusee, S., Robbins, V. H., and Baldwin, R. L. (1989) *Proc. Natl. Acad. Sci. U.S.A. 86*, 5286−5290.
2. Marqusee, S., and Baldwin, R. L. (1987) *Proc. Natl. Acad. Sci. U.S.A. 84*, 8898−8902.
3. Armstrong, K. M., Fairman, R., and Baldwin, R. L. (1993) *J. Mol. Biol. 230*, 284−291.
4. Huyghues-Despointes, B. M. P., Klingler, T. M., and Baldwin, R. L. (1995) *Biochemistry 34*, 13267−13271.
5. Shalongo, W., and Stellwagen, E. (1995) *Protein Sci. 4*, 1161−1166.
6. Chakrabartty, A., Doig, A. J., and Baldwin, R. L. (1993) *Proc. Natl. Acad. Sci. U.S.A. 90*, 11332−11336.
7. Chakrabartty, A., and Baldwin, R. L. (1995) *Adv. Protein Chem. 46*, 141−176.
8. Rohl, C. A., Chakrabartty, A., and Baldwin, R. L. (1996) *Protein Sci. 5*, 2623−2637.
9. Myers, J. K., Pace, C. N., and Scholtz, J. M. (1997) *Proc. Natl. Acad. Sci. U.S.A. 94*, 2833−2837.
10. Chakrabartty, A., Kortemme, T., and Baldwin, R. L. (1994) *Protein Sci. 3*, 843−852.
11. Creamer, T. P., and Rose, G. D. (1995) *Protein Sci. 4*, 1305−1314.
12. Srinivasan, R., and Rose, G. D. (1999) *Proc. Natl. Acad. Sci. U.S.A. 96*, 14258−14263.
13. Creamer, T. P., and Rose, G. D. (1992) *Proc. Natl. Acad. Sci. U.S.A. 89*, 5937−5491.
14. Luo, P., and Baldwin, R. L. (1999) *Proc. Natl. Acad. Sci. U.S.A. 96*, 4930−4935.
15. Avbelj, F., Luo, P., and Baldwin, R. L. (2000) *Proc. Natl. Acad. Sci. U.S.A. 97*, 10786−10791.
16. Vila, J. A., Ripoll, D. R., and Scheraga, H. A. (2000) *Proc. Natl. Acad. Sci. U.S.A. 97*, 13075−13079.
17. Garcia, A. E., and Sanbonmastu, K. Y. (2002) *Proc. Natl. Acad. Sci. U.S.A. 99*, 2782−2787.
18. Park, S. H., Shalongo, W., and Stellwagen, E. (1993) *Biochemistry 32*, 12901−12905.
19. Shalongo, W., Dugad, L., and Stellwagen, E. (1994) *J. Am. Chem. Soc. 116*, 2500−2507.
20. Rohl, C. A., and Baldwin, R. L. (1994) *Biochemistry 33*, 7760−7767.
21. Williams, S., Causgrove, T. P., Gilmanshin, R., Fang, K. S., Callender, R. H., Woodruff, W. H., and Dyer, R. B. (1996) *Biochemistry 35*, 691−697.
22. Martinez, G., and Millhauser, G. (1995) *J. Struct. Biol. 114*, 23−27.
23. Miick, S. M., Martinez, G., Fiori, W. R., Todd, A. P., and Millhauser, G. L. (1995) *Nature 377*, 257−257.
24. Graff, D. K., Pastrana-Rios, B., Venyaminov, S. Yu., and Prendergast, F. G. (1997) *J. Am. Chem. Soc. 119*, 11282−11294.
25. Decatur, S. M. (2000) *Biopolymers 45*, 180−185.
26. Decatur, S. M., and Antonic, J. (1999) *J. Am. Chem. Soc. 121*, 11914−11915.
27. Yoder, G., Pancoska, P., and Keiderling, T. A. (1997) *Biochemistry 36*, 15123−15133.
28. Silva, R. A. G. D., Kubelka, J., Bour, P., Decatur, S. M., and Keiderling, T. A. (2000) *Proc. Natl. Acad. Sci. U.S.A. 97*, 8318−8323.
29. Millhauser, G. L., Stenland, C. J., Hanson, P., Bolin, K. A., and vande Ven, F. J. M. (1997) *J. Mol. Biol. 267*, 963−974.
30. Mantsch, H. H., and Chapman, D. (1996) *Infrared Spectroscopy of Biomolecules*, Wiley-Liss, Chichester, U.K.
31. Surewicz, W., Mantsch, H. H., and Chapman, D. (1993) *Biochemistry 32*, 389−394.
32. Jackson, M., and Mantsch, H. H. (1995) *Crit. Rev. Biochem. Mol. Biol. 30*, 95−120.
33. Tadesse, L., Nazarbaghi, R., and Walters, L. (1991) *J. Am. Chem. Soc. 113*, 7036−7037.
34. Huang, C., Getahun, Z., Zhu, Y., Klemke, J. W., DeGrado, W. F., and Gai, F. (2002) *Proc. Natl. Acad. Sci. U.S.A. 99*, 2788−2793.
35. Venyaminov, S. Y., Hedstrom, J. F., and Prendergast, F. G. (2001) *Proteins: Struct., Funct., Genet. 45*, 81−89.
36. Huang, C. Y., Getahun, Z., Wang, T., DeGrado, W. F., and Gai, F. (2001) *J. Am. Chem. Soc. 123*, 12111−12112.
37. Manas, E. S., Getahun, Z., Wright, W. W., DeGrado, W. F., and Vanderkooi, J. M. (2000) *J. Am. Chem. Soc. 122*, 9883−9890.
38. Barber-Armstrong, W., Sridharan, M., and Decatur, S. M. (2002) in *Peptides: The wave of the future* (Lebl, M., and Houghten, R., Eds.) pp 367−368, Kluwer Press, Dordrecht, The Netherlands.
39. Diem, M. (1993) *Introduction to modern vibrational spectroscopy*, John Wiley and Sons, New York.

40. Sudha, T. S., Vijayakumar, E. K. S., and Balaram, P. (1983) *Int. J. Pept. Protein Res. 22*, 464−468.
41. Toniolo, C., Polese, A., Formaggio, F., Crisma, M., and Kamphuis, J. (1996) *J. Am. Chem. Soc. 118*, 2744−2745.
42. Manning, M. C., and Woody, R. W. (1991) *Biopolymers 31*, 569−586.
43. Karpen, M. E., De Haset, P. L., and Neet, K. E. (1992) *Protein Sci. 1*, 1333−1342.
44. Millhauser, G. L. (1995) *Biochemistry 34*, 3873−3877.
45. Sheinerman, F. B., and Brooks, C. L. (1995) *J. Am. Chem. Soc. 117*, 10098−10103.
46. Doig, A. J., MacArthur, M. W., Stapley, B. J., and Thornton, J. M. (1997) *Protein Sci. 6*, 147−155.
47. Rohl, C. A., and Doig, A. J. (1996) *Protein Sci. 5*, 1687−1696.
48. Kubelka, J., Silva, R. A. G. D., and Keiderling, T. A. (2002) *J. Am. Chem. Soc. 124*, 5325−5332.
49. Torii, H., and Tasumi, M. (1996) in *Infrared spectroscopy of biomolecules* (Mantsch, H. H., and Chapman, D., Eds.) pp 1−18, Wiley-Liss, New York.
50. Torii, H., and Tasumi, M. (1992) *J. Chem. Phys. 96*, 3379−3387.
51. Petukhov, M., Uegaki, K., Yumoto, N., and Serrano, L. (2002) *Protein Sci. 11*, 766−777.

BI026507Z